International Journal of Mathematics and
Computer Science, **16**(2021), no. 4, 1405–1421

Modeling COVID-19 Pandemic Outbreak using Fractional-Order Systems

Ramzi B. Albadarneh[1], **Iqbal M. Batiha**[2],
Adel Ouannas[3], **Shaher Momani**[4]

[1]Department of Mathematics
Faculty of Science
The Hashemite University
Zarqa, Jordan

[2]Department of Mathematics
Faculty of Science and Technology
Irbid National University
2600 Irbid, Jordan
and
Nonlinear Dynamics Research Center (NDRC)
Ajman University
Ajman 346, United Arab Emirates

[3]Department of Mathematics
Faculty of Science
Larbi Ben M'hidi University
Ouam El Bouaghi, Algeria

[4]Department of Mathematics
Faculty of Science
The University of Jordan
Amman 11942, Jordan
and
Nonlinear Dynamics Research Center (NDRC)
Ajman University
Ajman 346, United Arab Emirates

email: rbadarneh@hu.edu.jo, aqb9140074@fgs.ju.edu.jo,

Key words and phrases: COVID-19 pandemic, SEIR model, Caputo fractional-order operator, stability, basic reproductive number, elasticity indices.
AMS (MOS) Subject Classifications: 34A08, 37N25, 62P10.
ISSN 1814-0432, 2021, http://ijmcs.future-in-tech.net

ouannas.adel@univ-oeb.dz, s.momani@ju.edu.jo

(Received February 23, 2021, Accepted April 2, 2021)

Abstract

Recently, many nonlinear systems have been proposed to introduce the population dynamics of COVID-19. In this paper, we extend different physical conditions of the growth by employing fractional calculus. We propose a new fractional-order version for one of recently forms of the SEIR model. This version, which is established in view of the Caputo fractional-order differential operator, is numerically solved based on the Generalized Euler Method (GEM). Several numerical results reveal the impact of the fractional-order values on the established disease model. To help make a decline in the total of individuals infected by such pandemic, a new compartment is added to the proposed model; namely, the disease prevention compartment that includes the use of face masks, gloves and sterilizers. In view of such modification, it turned out that the performed addition to the fractional-order COVID-19 model yields a significant improvement in reducing the risk of COVID-19 spread.

1 Introduction

Like all other scientific fields, mathematical modeling plays a major role in facing a considerable number of tough epidemics like the COVID-19 epidemic. This field of research could principally contribute to realize the prevalence of the disease and understand its risk and assess its activity period and its influence on communities [1]. Such beneficial influences would undoubtedly support the policymakers who are responsible for recommending essential decisions and accountable for presenting suitable viewpoints, in assessing the social and economic strategies related to the epidemic evolution. It is common knowledge, in biomathematical modeling field, that any epidemiological mathematical model divides the whole community into multiple split compartments, for which each of them constitutes a certain health state. In particular, the Susceptible-Exposed-Infected-Recovered models (or simply SEIR models), which are the most fundamental common ones, played and still playing a leading role in describing several important biological phenomena, including the spread of different diseases.

In this paper, a new fractional-order version of a recent form of the SEIR model is established in light of the Caputo fractional-order differential operator. This fractional-order COVID-19 model is analyzed and solved using

the so-called Generalized Euler Method (GEM) numerically. In the final phases of this work, the proposed model is further modified through adding a new compartment, named the disease prevention compartment, to its original structure. It is confirmed that this compartment, which includes some of prevention manners, will yield a significant improvement in reducing the risk of COVID-19 spread.

2 Preliminaries and model formulation

In this section, some key definitions related to fractional calculus are briefly introduced together with some notions about the SEIR model that was proposed for dealing with the spread of COVID-19 pandemic.

Definition 2.1. *[2, 3] The Riemann Liouville fractional-order integral operator J^α of a function $f \in L_1[a,\ b]$ is defined by:*

$$J_t^\alpha f(t) = \frac{1}{\Gamma(\alpha)} \int_a^t (t-u)^{\alpha-1} f(u) du, \tag{2.1}$$

where $\alpha \in \mathbb{R}_+$ is the order of the operator, and $a \leq t \leq b$.

Definition 2.2. *[4, 5] The Caputo fractional-order differential operator ${}^C D^\alpha$ of a function f is defined by:*

$${}^C D_t^\alpha f(t) = \frac{1}{\Gamma(m-\alpha)} \int_a^t \frac{f^m(u)}{(t-u)^{\alpha+m-1}} du, \tag{2.2}$$

whenever the standard differential operator $D^m f \in L_1[a,\ b]$, where $\alpha \geq 0$ and $m = \lceil \alpha \rceil$.

Lemma 2.3. *[6] (Generalized Mean Value Theorem). Suppose that $\boldsymbol{Z}(t) \in C[a_1,\ a_2]$ and ${}^C D^\alpha \boldsymbol{Z}(t) \in C(a_1,\ a_2]$, where $0 < \alpha \leq 1$, then*

$$\boldsymbol{Z}(t) = \boldsymbol{Z}(a_1) + \frac{1}{\Gamma(\alpha)}\ {}^C D^\alpha \boldsymbol{Z}(\zeta)(t-a_1)^\alpha, \tag{2.3}$$

where $0 \leq \zeta \leq t$, $\forall t \in (a_1,\ a_2]$.

Remark 2.4. *[6] Suppose that $\boldsymbol{Z}(t) \in C[0,\ a_2]$ and ${}^C D^\alpha \boldsymbol{Z}(t) \in C(0,\ a_2]$, where $0 < \alpha \leq 1$. In view of the above Lemma, one can conclude that if ${}^C D^\alpha \boldsymbol{Z}(t) \geq 0$, $\forall t \in (0,\ a_2]$, then $\boldsymbol{Z}(t)$ will be a non-decreasing vector-valued function, while if ${}^C D^\alpha \boldsymbol{Z}(t) \leq 0$, $\forall t \in (0,\ a_2]$, then such function will be non-increasing one.*

Table 1: Initial values of the SEIR model.

Variable compartment	Value
$E(0)$	20000
$I(0)$	1
$N(0)$	10×10^6
$R(0)$	1
$S(0)$	$N(0) - E(0) - 1$

In [7], Carcione et al. implemented an SEIR model to compute the infected population and the number of casualties of the COVID-19 epidemic. In particular, they deduced some analysis results of the model by varying the parameters and initial conditions. However, Figure 1, illustrates the block diagram of all compartments of such model including all their conversion relationships.

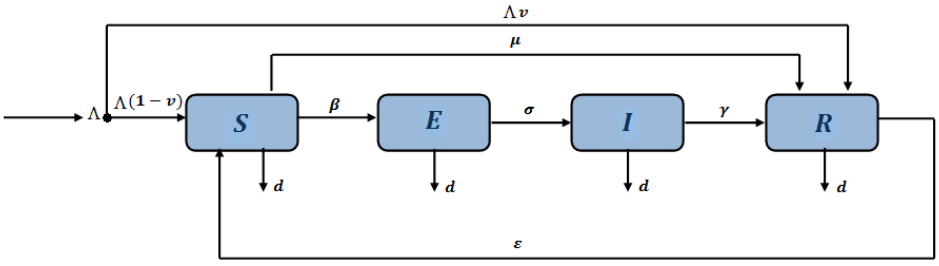

Figure 1: A compartment diagram for a modification of SEIR model.

The initial values along with all parameters of the dynamic model have been fitted according to the raw epidemic data given in [7], and by considering N as the total number of live humans in the system at time t. In particular, Tables 1 and 2 show all initial conditions and parameters embedded in the model at hand, respectively.

In general, the mathematical model, which has been established in [7, 8]

Table 2: Description of parameters of the SEIR model.

Parameter	**Meaning**	**Value**
Λ	Per-capita birth rate	–
d	Per-capita natural death rate	–
ε	Virus induced average fatality rate	0.006
β	Probability of disease transmission per contact	0.85
μ	Vaccination Rate	0
σ	Rate of progression from exposed to infected	0.0049
γ	Recovery rate of infected individuals	0.125
v	Vaccination proportion (Newborns)	0

as an implementation of the SEIR model, has the following form:

$$\begin{aligned}
\frac{dS}{dt} &= \Lambda - vN - \beta\frac{SI}{N} - dS + \varepsilon R - \mu S \\
\frac{dE}{dt} &= \beta\frac{SI}{N} - (\sigma + d)E \\
\frac{dI}{dt} &= \sigma E - (\gamma + d + \varepsilon)I \\
\frac{dR}{dt} &= \gamma I - (d + \varepsilon)R + \mu S.
\end{aligned} \tag{2.4}$$

If one assumes that the individuals in R are immune; i.e., the individuals in R will not never return to S for the duration of the model, then εR vanishes. Besides, if we assume that there is no effective vaccine so far, then v and μ will also vanish from the model, as reported in Table 2. Hence, the model in (2.4) will take the following form:

$$\begin{aligned}
\frac{dS}{dt} &= \Lambda - \beta\frac{SI}{N} - dS \\
\frac{dE}{dt} &= \beta\frac{SI}{N} - (\sigma + d)E \\
\frac{dI}{dt} &= \sigma E - (\gamma + d + \varepsilon)I \\
\frac{dR}{dt} &= \gamma I - dR.
\end{aligned} \tag{2.5}$$

For the purpose of introducing the proposed COVID-19 model in this work, which relies on the Caputo operator, we have to fractionalize system (2.5) as

follows:

$$\begin{aligned} {}^{C}D_t^{\alpha}S(t) &= \Lambda - \beta\frac{SI}{N} - dS \\ {}^{C}D_t^{\alpha}E(t) &= \beta\frac{SI}{N} - (\sigma + d)E \\ {}^{C}D_t^{\alpha}I(t) &= \sigma E - (\gamma + d + \varepsilon)I \\ {}^{C}D_t^{\alpha}R(t) &= \gamma I - dR. \end{aligned} \tag{2.6}$$

Since $N = S + E + I + R$, one can easily obtain the following assertion:

$${}^{C}D_t^{\alpha}N(t) = \Lambda - dN - \varepsilon I. \tag{2.7}$$

This means that N is not constant, which implies that $R(t)$ can be obtained using the following relation:

$$R(t) = N(t) - S(t) - E(t) - I(t). \tag{2.8}$$

In conclusion of this section, an equivalent model to model (2.6) can be proposed based on the previous discussion. This model has the following form:

$$\begin{aligned} {}^{C}D_t^{\alpha}S(t) &= \Lambda - \beta\frac{S(t)I(t)}{N(t)} - dS(t) \\ {}^{C}D_t^{\alpha}E(t) &= \beta\frac{S(t)I(t)}{N(t)} - (\sigma + d)E(t) \\ {}^{C}D_t^{\alpha}I(t) &= \sigma E(t) - (\gamma + d + \varepsilon)I(t) \\ {}^{C}D_t^{\alpha}N(t) &= \Lambda - dN(t) - \varepsilon I(t), \end{aligned} \tag{2.9}$$

subject to initial conditions given in Table 1. The numerical solution of system (2.9) can be obtained using one of significant numerical schemes, namely the GEM. To get a full description about this method and how it can be employed in actual research, we refer the reader to [9]. However, Figure 2 shows approximate solutions for all classes of system (2.9) according to the initial states given in Table 1, and according to the balanced assumption that assumes the births and the natural deaths are balanced (i.e., Λ and d are assumed 0). Actually, this figure represents the whole size for each of susceptible-, exposed-, infected-, and recovered-people over the time t, which have been performed in view of different values of α. In view such figure, one may observe that any variation in the fractional-order values can affect on the current disease model.

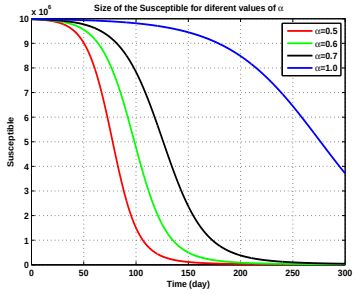

(a) Size of Susceptible people S over time t.

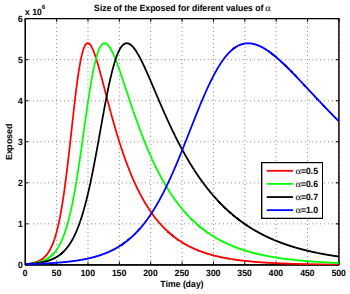

(b) Size of Exposed people E over time t.

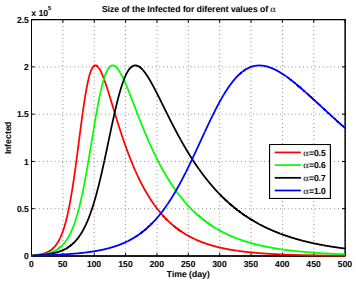

(c) Size of Infected people I over time t.

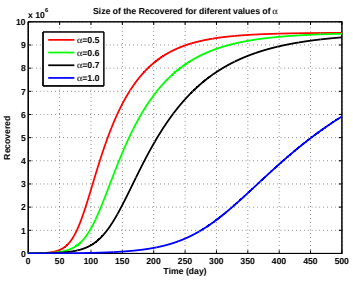

(d) Size of Recovered people R over time t.

Figure 2: Size of all classes over the time t (in days) for system (2.9) in view of different values of α.

3 Stability analysis

This section is dedicated to deduce several stability analysis results associated with the fractional-order COVID-9 model established in (2.9). These results are associated with the equilibrium points, the positivity solution of such system, and determining the basic reproductive number R_0 as well as its elasticity indices.

3.1 Positivity solution of the model

In this part, we focus on providing a useful result that associated with showing that the solution $\mathbf{Z}(t) = [S(t),\ E(t),\ I(t),\ R(t)]^T$ of system (2.6) subject to the initial conditions $\mathbf{Z}(0) = [S(0),\ E(0),\ I(0),\ R(0)]^T \in \mathbb{R}^4_+ := \{\mathbf{Z}(t) \in \mathbb{R}^4 :\ \mathbf{Z}(t) \geq 0\}$ is non-negative solution.

Theorem 3.1. *There exists a unique solution* $\boldsymbol{Z}(t) = [S(t),\ E(t),\ I(t),\ R(t)]^T$ *of system (2.6) subject to the initial condition* $\boldsymbol{Z}(0) = [S(0),\ E(0),\ I(0),\ R(0)]^T \in \mathbb{R}^4_+ := \{\boldsymbol{Z}(t) \in \mathbb{R}^4 :\ \boldsymbol{Z}(t) \geq 0\}$, *and this solution will still be in* $\mathbb{R}^4_+$.

Proof. Referring to some novel results deduced by Lin in [10] leads us to definitely identify a unique solution $\mathbf{Z}(t)$ on $(0,\ \infty)$ for system (2.6) subject to the initial condition $\mathbf{Z}(0)$. On the other hand, in order to show that the domain $\mathbb{R}^4_+$ is, indeed, positively invariant region, we have to observe the following assertions:

$$\begin{aligned} &{}^{C}D^{\alpha}S(t)|_{S=0} = \Lambda \geq 0,\ {}^{C}D^{\alpha}E(t)|_{E=0} = \beta\frac{SI}{N} \geq 0, \\ &{}^{C}D^{\alpha}I(t)|_{I=0} = \sigma E \geq 0,\ {}^{C}D^{\alpha}R(t)|_{R=0} = \gamma I \geq 0. \end{aligned} \tag{3.10}$$

Thus, based on the above two results, one can deduce that $\mathbb{R}^4_+$ is an invariant set, and this completes the proof. □

3.2 The equilibrium points of the model

It could be argued that determining the equilibrium points of any epidemiological model is considered one of the main aspects that needed to study its stability analysis. Actually, there are two main kinds of those points that could be classified according to absence of the infection; the Disease-Free Equilibrium (DFE) point and the Endemic Equilibrium (EE) point. For instance, to find the DFE point for system (2.9), we first put all right-hand sides of all system's equations to be equal 0, along with assuming that $I = 0$ in that system. This exactly has led us to the following point:

$$\bar{\mathbf{X}}_{DFE} = (\frac{\Lambda}{d}, 0, 0, \frac{\Lambda}{d}). \tag{3.11}$$

On the other hand, if one considers $I \neq 0$, then the following EE point will be gained:

$$\bar{\mathbf{X}}_{EE} = (S^*, E^*, I^*, N^*), \tag{3.12}$$

where

$$\begin{aligned} &S^* = \left(\frac{\sigma\Lambda - (\sigma+d)(\gamma+d+\varepsilon)}{\sigma d}\right) I^*,\ E^* = \left(\frac{\gamma+d+\varepsilon}{\sigma}\right) I^*, \\ &N^* = \left(\frac{\Lambda-\varepsilon}{d}\right) I^*,\ \text{and}\ I^* = \frac{\Lambda(\sigma+d)(\gamma+d+\varepsilon) - \sigma\beta\Lambda}{(\varepsilon-\beta)(\sigma+d)(\gamma+d+\varepsilon)}. \end{aligned} \tag{3.13}$$

It is worth noting that the benefit of obtaining these equilibrium points stems from its utmost importance in exploring some other stability results that relate to the so-called basic reproductive number R_0, which will be considered in the next subsection.

3.3 Basic reproductive number

The basic reproductive number R_0 indicates to the average number of the secondary cases generated from initial infective cases within a population with no immunity to the disease [11]. Such critical scale has increasingly being a principal quantity used for determining the force of required interferences for controlling the epidemics. In epidemic mathematical modeling, it is common knowledge that if $R_0 < 1$, then there is an absence of epidemics in natural populations. On the contrary, if $R_0 > 1$, then the disease will increasingly spread in the susceptible population. However, the method to determine such scale requires to find the spectral radius of the next generation matrix or the largest absolute value of its eigenvalues (i.e., $R_0 = \rho(K)$, where K is the next generation matrix) [12]. The matrix K consists typically of two components F and V^{-1}, in which:

$$F = \left[\frac{\partial F_i(\bar{\mathbf{X}}_{DFE})}{\partial t_j}\right] \text{ and } V = \left[\frac{\partial V_i(\bar{\mathbf{X}}_{DFE})}{\partial t_j}\right], \tag{3.14}$$

where F_i indicate the flux of newly infected in compartment z_i, and V_i indicate to other leaving/entering fluxes associated with the compartment z_i, for $i, j = 1, 2, ..., m$, in which m is the number of compartments established in the model.

In view of the previous discussion, one can compute R_0 for our proposed fractional-order model given in (2.9) by first finding the two major matrices F and V^{-1}, which would be as follows:

$$F = \begin{bmatrix} 0 & \beta \\ 0 & 0 \end{bmatrix} \text{ and } V^{-1} = \begin{bmatrix} \frac{1}{\sigma+d} & 0 \\ \frac{\sigma}{(\sigma+d)(\gamma+d+\varepsilon)} & \frac{1}{\gamma+d+\varepsilon} \end{bmatrix}. \tag{3.15}$$

Consequently, the next generation matrix would be in the form:

$$K = FV^{-1} = \begin{bmatrix} \frac{\beta\sigma}{(\sigma+d)(\gamma+d+\varepsilon)} & \frac{\beta}{\gamma+d+\varepsilon} \\ 0 & 0 \end{bmatrix}. \tag{3.16}$$

This definitely leads us to deduce the following form of R_0:

$$R_0 = \rho(K) = \frac{\beta\sigma}{(\sigma+d)(\gamma+d+\varepsilon)}. \tag{3.17}$$

In the same context, the above assertions pave the way to gain further result associated with the local stability analysis of DFE point.

Theorem 3.2. *The DFE point $\bar{\boldsymbol{X}}_{DFE}$ of system (2.9) is locally stable if $R_0 < 1$.*

Proof. To begin with the proof of this theorem, one needs to find the corresponding Jacobian matrix of system (2.9), which would be in the following form:

$$J = \begin{bmatrix} -\left(d + \beta\frac{I}{N}\right) & 0 & -\beta\frac{S}{N} & \beta\frac{IS}{N^2} \\ \beta\frac{I}{N} & -(d+\sigma) & \beta\frac{S}{N} & -\beta\frac{IS}{N^2} \\ 0 & \sigma & -(\gamma+d+\varepsilon) & 0 \\ 0 & 0 & -\varepsilon & -d \end{bmatrix}. \tag{3.18}$$

Thus, the Jacobian matrix at the DFE point $\bar{\mathbf{X}}_{DFE}$ will be in the following form:

$$J(\bar{\mathbf{X}}_{DFE}) = \begin{bmatrix} -d & 0 & -\beta & 0 \\ 0 & -(d+\sigma) & \beta & 0 \\ 0 & \sigma & -(\gamma+d+\varepsilon) & 0 \\ 0 & 0 & -\varepsilon & -d \end{bmatrix}. \tag{3.19}$$

After performing some long calculations, we have obtained all eigenvalues of $J(\bar{\mathbf{X}}_{DFE})$ to be as follows: $\lambda_{1,2} = -d < 0$, whereas $\lambda_3, \lambda_4 < 0$, only if $R_0 < 1$. Now, due to all eigenvalues of $J(\bar{\mathbf{X}}_{DFE})$ are less than 0, and from the perspective that asserts that the stability of the model formulated using ODEs implies also its stability in its fractional-order case (see [13]), we obtain the desired result. □

3.4 Elasticity index of R_0

The local sensitivity analysis illustrates how the basic reproductive number R_0 will be impacted in response to some changes that may occur to the parameters of the model [12, 14]. The so-called elasticity index, which represents a normalization of the sensitivity index, is defined as the ratio of the relative change in the variable to the relative change in the parameter. The value of R_0 will be increased, if elasticity index is positively increased, and vice versa [12, 14]. However, the general expression of the elasticity index with respect to the parameter ϱ can be represented as follows:

$$\Upsilon_{\varrho}^{R_0} = \frac{\partial R_0}{\partial \varrho} \times \frac{\varrho}{R_0}. \tag{3.20}$$

In accordance with the parameters' values given in Table 2, we exhibit in Table 3 the baseline parameter values and their corresponding elasticity indices for the fractional-order COVID-19 model given in (2.9), whereas Figure 3 summarizes all these indices.

Table 3: Baseline parameter values and elasticity indices for system (2.9).

Parameter	**Elasticity**	**Numerical Elasticity**
β	$\Upsilon_{\beta}^{R_0} = 1$	1
σ	$\Upsilon_{\sigma}^{R_0} = 1 - \frac{\sigma(2\sigma+d+\gamma+\varepsilon)}{(\sigma+d)(\gamma+\sigma+\varepsilon)}$	0.9999
d	$\Upsilon_{d}^{R_0} = \frac{-d(\gamma+\sigma+\varepsilon)}{\sigma+d}$	0
γ	$\Upsilon_{\gamma}^{R_0} = \frac{-\gamma}{\gamma+\sigma+\varepsilon}$	-0.9197
ε	$\Upsilon_{\varepsilon}^{R_0} = \frac{-\varepsilon}{\gamma+\sigma+\varepsilon}$	-0.0442

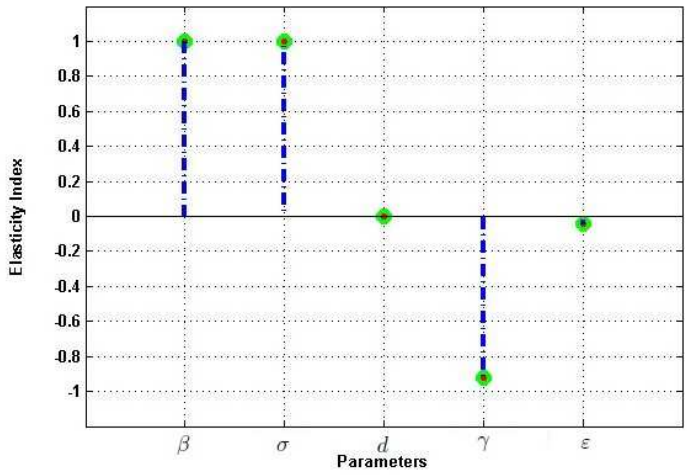

Figure 3: Bar graph illustrating the elasticity index for each parameter of system (2.9).

In view of the results exhibited in Table 3 and Figure 3, one can deduce that the parameter with most impact on the calculation of R_0 is the probability of transmission per contact β. In other words, any increase in β will correspond to major increase in the probability of humans becoming infected with COVID-19, see Figures 4(a). On the other hand, the sensitive parameter on R_0 with the least impact is the recovery rate of the infected individuals γ. That is, any increase in such parameter will correspond to a major decrease in the probability of humans becoming infected with COVID-19, see Figure 4(b).

(a) Effect of the parameter β on R_0. (b) Effect of the parameter γ on R_0.

Figure 4: Effect of the most and least impact parameters on R_0.

4 Adding the disease prevention compartment to the model

In view of lack of comprehensive vaccines in the pandemic period of COVID-19 outbreak, many countries have adopted a highest control measures reasonably practicable and the maximum disease prevention strategies for the purpose of controlling the spread of infection [11]. Such interventions or strategies have shown their roles in lowering the risk of infection from confirmed or possible Coronavirus (COVID-19) infection or even the risk of death. Some of these strategies include isolation, quarantine and lockdowns. In this section, we intend to formulate a modification for the fractional-order COVID-19 model given in (2.9) by adding a new compartment namely the disease prevention compartment that includes the use of face masks, gloves and sterilizers. The main motivation of performing this task is to prove the extreme significance of adhering to these disease prevention tools. The new compartmental diagram of the modified model for system (2.9) with its all corresponding equations is exhibited in Figure 5.

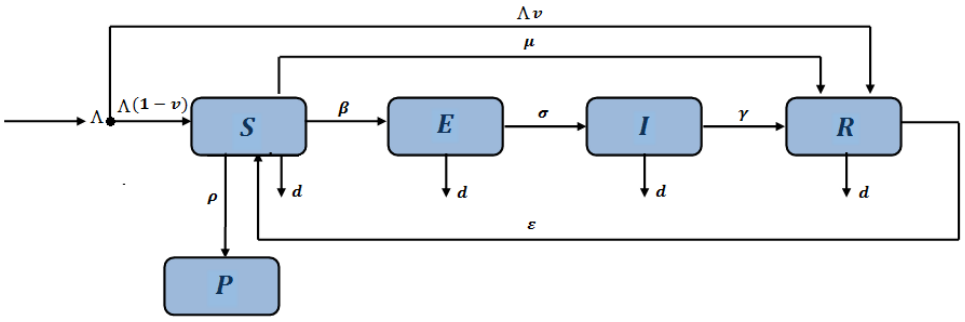

Figure 5: A compartmental diagram of the new modification for the fractional-order COVID-19 model.

Actually, this compartmental diagram necessitates one to develop system (2.9) to be in the following form:

$$\begin{aligned}
&{}^{C}D_t^{\alpha}S(t) = \Lambda - \beta\frac{S(t)I(t)}{N(t)} - dS(t) - \omega S(t)\\
&{}^{C}D_t^{\alpha}P(t) = \omega S(t)\\
&{}^{C}D_t^{\alpha}E(t) = \beta\frac{S(t)I(t)}{N(t)} - (\sigma + d)E(t)\\
&{}^{C}D_t^{\alpha}I(t) = \sigma E(t) - (\gamma + d + \varepsilon)I(t)\\
&{}^{C}D_t^{\alpha}N(t) = \Lambda - dN(t) - \varepsilon I(t),
\end{aligned} \tag{4.21}$$

where $P(t)$ is the disease prevention compartment and ω is the ratio of people who adhere to the disease prevention tools.

In order to examine the modified fractional-order COVID-19 model, several comparison numerical simulations are performed between the two vector-valued solutions of the two systems given in (2.9) and (4.21). These comparisons consider the same initial values given in Table 1 with $P(0) = 100$, and the same parameters' values given in Table 2. Besides, we assume that the ratio of people who adhere to the disease prevention tools as $\omega = 0.0025$. The overall results of these comparisons are shown in Figure 6. These results definitely reveal that although the performed addition requires a slight modification to the models equations, it has given a significant improvement in reducing the number of susceptible people from the disease, and hence reducing the number of exposed and infected people. This would undoubtedly decrease the risk of COVID-19 spread.

In view of the aforementioned comparison results, the effect of the parameter ω has shown its significant role in reducing the number of susceptible people from the disease. This relation between ω and S can be further explored by considering the next result.

Proposition 4.1. *The susceptible class $S(t)$ approaches 0 as the parameter ω approaches 1.*

Proof. If one supposes that $\omega \to 1$, then the second equation of system (4.21) will be ${}^{C}D_t^{\alpha}P(t) = S(t)$. Consequently, the first equation of such system will be in the following form:

$${}^{C}D_t^{\alpha}S(t) + dS(t) = \Lambda - \beta\frac{S(t)I(t)}{N(t)}. \tag{4.22}$$

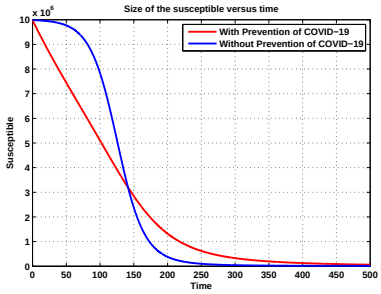

(a) Size of Susceptible people S over time t.

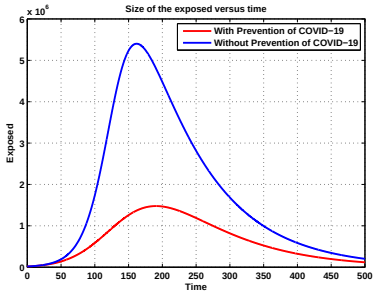

(b) Size of Exposed people E over time t.

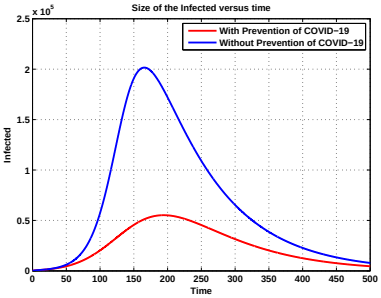

(c) Size of Infected people I over time t.

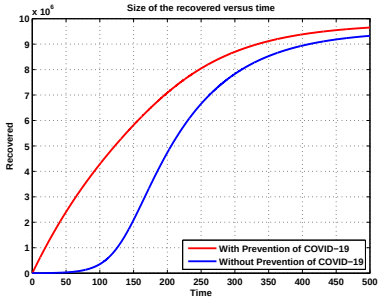

(d) Size of Recovered people R over time t.

Figure 6: Comparison results between the approximate solutions of (3.13) and (4.21) with $\alpha = 0.95$.

Combining this equation with the third equation of system (4.21) yields:

$$ {}^{C}D_t^{\alpha} S(t) + dS(t) = \Lambda - ({}^{C}D_t^{\alpha} E(t) + (\sigma + d)E(t)). \tag{4.23} $$

Suppose, to the contrary, that $S(t) \nrightarrow 0$. That is, $S(t) > 0$, $\forall t$. Together with (4.23), this implies the following:

$$ {}^{C}D_t^{\alpha} E(t) + (\sigma + d)E(t)) < \Lambda. \tag{4.24} $$

Together with the third equation of the system, this inequality implies $\beta \frac{S(t)I(t)}{N(t)} < \Lambda$, which contradicts its converse ($\beta \frac{S(t)I(t)}{N(t)} < \Lambda$) that can be deduced easily from the first equation of the system. The desired result follows, □

The above result can be further asserted by some numerical simulations shown in Figure 7. In particular, part (a) shows that the susceptible class will vanish once the people in such class adhere to the disease prevention tools that include face masks, gloves and sterilizers, while part (d) of the same figure shows that the size of the recovered people will increase once they also

adhere the aforesaid tools. In general, the modified fractional-order model given in (4.21) can assist the health authorities with fighting the COVID-19 outbreak, and it may also let us to say that an ounce of prevention is better than a pound of cure.

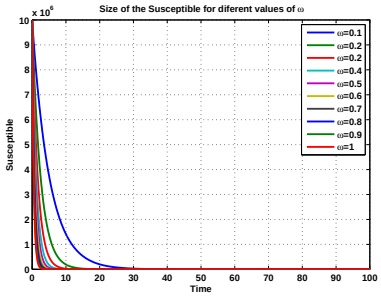

(a) Size of Susceptible people S over time t.

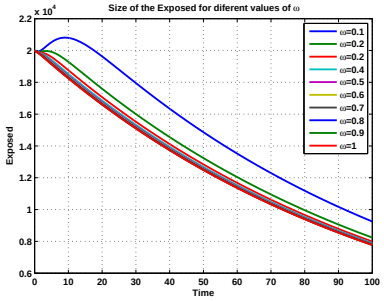

(b) Size of Exposed people E over time t.

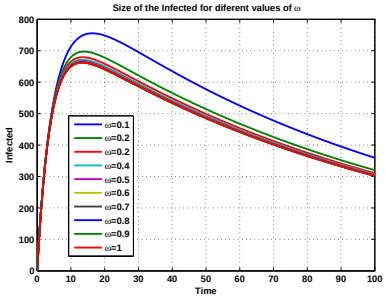

(c) Size of Infected people I over time t.

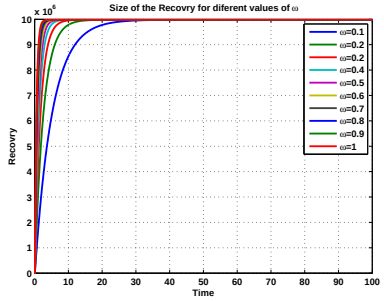

(d) Size of Recovered people R over time t.

Figure 7: Numerical results of the vector-valued solutions of model (4.21) with $\alpha = 0.9$, for different values of ω.

5 Conclusion

In this work, a novel fractional-order SEIR models for spread of COVID-19 pandemic has been established in view of the Caputo fractional-order operator. The graphical simulation results obtained from using the generalized Euler method have revealed that any varying in the fractional-order values will affect on the established disease model. The proposed fractional-order COVID-19 model has been addressed in terms of its equilibrium points, its positivity solution, and its basic reproductive number R_0 with its elasticity indices. For instance, in view of all computed elasticity indices of R_0 together with some graphical results, it has been shown that the probability of

transmission per contact is the most impact parameter on the calculation of R_0, while the least impact sensitive parameter on such number is the recovery rate of the infected individuals. Finally, the fractional-order COVID-19 model has been further modified by adding a new compartment namely the disease prevention compartment that includes the use of face masks, gloves and sterilizers. It also has been examined by performing several comparison simulations between its numerical solution and the other numerical solution obtained previously for the original model. Such comparison simulations have revealed that the performed modification of the fractional-order COVID-19 model yields a significant improvement in reducing the risk of COVID-19 spread.

References

[1] R. Almeida, A. M. C. Brito da Cruz, N. Martins, M. T. Monteiro, *An epidemiological MSEIR model described by the Caputo fractional derivative,* International Journal of Dynamics and Control, **7,** (2019), 776–784.

[2] I. M. Batiha, R. B. Albadarneh, S. Momani, I. H. Jebril, *Dynamics analysis of fractional-order Hopfield neural networks,* International Journal of Biomathematics, **13,** no. 8, (2020), 2050083, DOI:10.1142/S1793524520500837.

[3] R. B. Albadarneh, I. M. Batiha, N. Tahat, A. K. Alomari, *Analytical Solutions of Linear and Non-linear Incommensurate Fractional-order Coupled Systems,* Indonesian Journal of Electrical Engineering and Computer Science, **21,** no. 2, (2021), 776–790, DOI: 10.11591/ijeecs.v21.i2.

[4] R. B. Albadarneh, I. M. Batiha, M. Zurigat, Numerical solutions for linear fractional differential equations of order $1 < \alpha < 2$ using finite difference method (FFDM), Journal of Mathematics and Computer Science, **16,** no. 1, (2016), 103–111, DOI: 10.22436/jmcs.016.01.11

[5] A. K. Alomari, G. A. Drabseh, M. F. Al-Jamal, R. B. Albadarneh, Numerical simulation for fractional phi-4 equation using homotopy Sumudu approach, International Journal of Simulation and Process Modelling, **16,** no. 1,(2021), 26–33, DOI: 10.1504/IJSPM.2021.113072.

[6] P. A. Naika, J. Zua, K. M. Owolabi, *Global dynamics of a fractional order model for the transmission of HIV epidemic with optimal control,* Chaos, Solitons & Fractals, **138,** (2020), 10982.

[7] J. M. Carcione, J. E. Santos, C. Bagaini, J. Ba, *A Simulation of a COVID-19 Epidemic Based on a Det erministic SEIR Model,* Front Public Health, **8,** (2020), 230.

[8] M. B. Trawicki, *Deterministic seirs epidemic model for modeling vital dynamics, vaccinations, and temporary immunity,* Mathematics, **5,** no. 7, (2017).

[9] Y. Y. Y. Yameni Noupoue, Tandoğdu, M. Awadalla, *On numerical techniques for solving the fractional logistic differential equation,* Adv. Differ. Equ., (2019), 108.

[10] W. Lin, *Global existence theory and chaos control of fractional differential equations,* J. Math. Anal. Appl., **332,** (2007), 709–726.

[11] S. Pengpeng, C. Shengli, F. Peihua, *SEIR transmission dynamics model of 2019 nCoV coronavirus with considering the weak infectious ability and changes in latency duration,* medRxiv, (2020), DOI: 10.1101/2020.02.16.20023655.

[12] P. van den Driessche, *Reproduction numbers of infectious disease models,* Infectious Disease Modeling, **2,** no. 3, 288–303.

[13] M.R. Islam, A. Peace, D. Medina, T. Oraby, *Integer versus fractional order SEIR deterministic and stochastic models of measles,* Int. J. Environ. Res. Public Health, **17,** 6, (2020).

[14] S. Bañuelos, M. V. Martinez, C. Mitchell, A. Prieto-Langarica, *Using mathematical modeling to investigate the effect of the sexual behavior of asymptomatic individuals and vector control measures on Zika,* Letters in Biomathematics, **6,** no. 1, (2019), 1–19, DOI: 10.1080/23737867.2019.1624631.